Journal of Functional Foods 64 (2020) 103640

Contents lists available at ScienceDirect

Journal of Functional Foods

journal homepage: www.elsevier.com/locate/jff

The anthocyanin extracts from purple-fleshed sweet potato exhibited anti-photoaging effects on ultraviolent B-irradiated BALB/c-nu mouse skin

Qi Zhi[a], Lin Lei[a], Fuhua Li[a,b], Jichun Zhao[a,b], Ran Yin[c], Jian Ming[a,b,*]

[a] College of Food Science, Southwest University, Chongqing 400715, People's Republic of China
[b] Research Center of Food Storage & Logistics, Southwest University, Chongqing 400715, People's Republic of China
[c] Ernest Mario School of Pharmacy, Rutgers University, 160 Frelinghuysen Rd, Piscataway Township, NJ 008854, USA

ARTICLE INFO

Keywords:
Purple-fleshed sweet potato
Anthocyanin
Anti-photoaging
MAPK
NF-κB

ABSTRACT

This study investigated the effect of anthocyanin extracts from purple-fleshed sweet potato (PSP-AE) on ultraviolet B (UVB)-induced skin photoaging in BALB/c-nu mice. UPLC-QTOF-MS analysis showed six compounds were identified from PSP-AE. Administration of PSP-AE ameliorated the UVB-irradiated macroscopic and histopathological lesions of the skin *via* suppressing epidermal hyperplasia and collagen degradation, while improving the content of skin moisture and hydroxyproline. Additionally, PSP-AE inhibited the UVB-induced oxidative stress and increased the antioxidant enzyme activities. Results showed PSP-AE inhibited the UVB-irradiated levels of pro-inflammatory cytokines, such as tumor necrosis factor α and interleukin 6. Furthermore, Western blot analysis revealed PSP-AE remarkably decreased the protein levels of phosphorylated c-Jun-Nterminal kinase, extracellular signal-regulated kinase, and p38. Likewise, UVB induced nuclear translocation of nuclear factor kappa-B and the expression of matrix metalloproteinase 1 were diminished by pretreatment of PSP-AE. Therefore, PSP-AE had the potential to attenuate the UVB-irradiated skin oxidative stress and inflammatory response.

1. Introduction

Skin aging, namely functional and esthetic changes of skin, is a complex and multifactorial process caused by both intrinsic and extrinsic factors, such as solar ultraviolet B (UVB) radiation. Excessive UVB skin exposure can cause sunburn, edema, erythema, hyperplasia, melanoma and even carcinogenesis (Ye, Sun-Waterhouse, You, & Abbasi, 2017). UVB-induced premature aging, known as photoaging, is associated with the increasing degradation of the extracellular matrix (ECM) in the skin. The degradation of the ECM is predominantly attributable to alter intracellular signaling pathways including collagen degradation and stimulation of matrix metalloproteinases (MMPs) (Kwak, Yang, Shin, & Chung, 2018). MMPs can be activated by UVB-induced oxidative stress and inflammatory response (Masaki, 2010). Excessive generation of reactive oxygen species (ROS), produced from UVB-induced oxidative stress, leads to the incidence of lipid peroxidation and inflammation. Additionally, accumulating evidences indicated that UVB-induced ROS could promote the production of pro-inflammatory cytokines such as tumor necrosis factor-α (TNF-α), interleukin-1β (IL-1β) and interleukin-6 (IL-6), which were directly related with the activation of activator protein-1 (AP-1), the mitogen-activated protein kinases (MAPK) and the nuclear factor-κB (NF-κB) signaling pathways (Rabe, Mamelak, McElgunn, Morison, & Sauder, 2006). These effects ultimately lead to the degradation of collagen and the formation of photoaging. The medical treatment of skin photoaging is mainly focused on antioxidants (vitamin, plant and marine extracts), anti-inflammatory agents (antiretinoic acid, aspirin, and glucocorticoid) and traditional Chinese medicine (panax ginseng glycosides, baicalin, and ganoderma lucidum polysaccharide) (Poon, Kang, & Chien, 2015). Research showed that the chemically synthesized drugs such as antiretinoic acid and aspirin may irritate the skin and need long-term consumption (Cho et al., 2005; Uliasz & Spencer, 2004). However, an abundant source of plant and marine extracts play important roles in preventing skin photoaging with minimal side effects (Kim et al., 2016).

Abbreviations: AP-1, Activator protein-1; CAT, Catalase; COX-2, Cyclo-oxyge-nase 2; ECM, Extracellular matrix; ERK, Extracellular signal-regulated kinase; GSH-Px, Glutathione peroxidase; Hyp, Hydroxyproline; JNK, C-Jun-Nterminal kinase; IL-1β, Interleukin-1β; IL-6, Interleukin-6; MAPK, Mitogen-activated protein kinases; MDA, Malondialdehyde; MMPs, Matrix metalloproteinases; NF-κB, Nuclear factor-κB; PBS, Phosphate buffer saline; PSP-AE, Anthocyanin extracts from purple-fleshed sweet potato; ROS, Reactive oxygen species; SOD, Superoxide dismutase; TNF-α, Tumor necrosis factor-α; UVB, Ultraviolet B

* Corresponding author at: College of Food Science, Southwest University, Tiansheng Road 2, Chongqing 400715, People's Republic of China.
E-mail address: food_mj@swu.edu.cn (J. Ming).

https://doi.org/10.1016/j.jff.2019.103640
Received 28 August 2019; Received in revised form 13 October 2019; Accepted 16 October 2019
Available online 30 October 2019

Recently, an increasing attention has been focused on natural plant phenolics, including plant flavonoids, to prevent the UVB-irradiated skin damages. Many studies have demonstrated that natural plant flavonoids can effectively reduce the incidence of skin photoaging through their photoprotective, antioxidant, and anti-inflammatory activities (Bosch et al., 2015; Lee et al., 2018; Ren et al., 2016; Svobodova, Psotova, & Walterova, 2003). Anthocyanin, widely distributed in vegetables, fruits, beans and cereals, have various biological activities including antioxidant, anti-inflammatory and anti-microbial capacities (Khoo, Azlan, Tang, & Lim, 2017). In addition to these properties, anthocyanin extracted from natural plants including black soybean, grapes and berries have been demonstrated to possess the effect of delaying the aging of organisms (Khoo et al., 2017). Cyanidin-3-glucoside (C3G), a major constituent of anthocyanin, is commonly found in pigmented fruits and vegetables, especially in berries and grapes. It has been reported that G3G could inhibit the UVB-induced skin edema, epidermal hyperplasia and leukocyte infiltration (Pratheeshkumar et al., 2014). Delphinidin, the main aglycon of anthocyanin, can decrease UVB-induced inflammation *via* mediating MAPKK4 and PI-3 kinase activities to suppress *cyclo*-oxyge-nase 2 (COX-2) overexpression (Kwon et al., 2009). Black rice extracts, contained antioxidative flavonoid components such as cyanidin-3-O-β-D-glycoside, were found to attenuate UV-induced MMPs overproduction and suppress the activation of AP-1 to protect skin from ECM damage (Han, Kang, Oh, Lee, & Chung, 2018). Purple sweet potato, a rice source of stable anthocyanin, is one of the major crops widely distributed in the world (Han et al., 2018). The major active components of purple sweet potato anthocyanin were cyanidin or paeoniflorin derivatives acylated with caffeic acid, ferulic acid and *p*-hydroxybenzoic acid (Kim, Kim, et al., 2012). The anthocyanin extracts from purple sweet potato (PSP-AE) possessed many bioactive properties such as antioxidant, antimicrobial, anti-inflammatory and anticancer activities, as well as alleviation of cardiovascular diseases (Khoo et al., 2017). However, information about the protective effect of PSP-AE on UVB-induced skin photoaging is limited.

Thus, this study aims to evaluate the protective effects of PSP-AE on UVB-irradiated oxidative stress and inflammation associated with photoaging using BALB/c-nu mouse skin model, with focus on the MAPK and NF-κB signaling pathways.

2. Materials and methods

2.1. Chemicals and reagents

The assay kits for superoxide dismutase (SOD), glutathione peroxidase (GSH-Px), catalase (CAT), malondialdehyde (MDA), hydroxyproline (Hyp) and protein extraction kits were bought from Nanjing Jiancheng Bioengineering Co., Ltd (Nanjing, China). TNF-α and IL-6 ELISA assay kits were purchased from Huijia Biotechnology Co., Ltd (Xiamen, China). The BCA protein assay kits and the antibodies specific for c-Jun-Nterminal kinase (JNK), phosphorylated JNK (p-JNK), extracellular signal-regulated kinase (ERK), phosphorylated ERK (p-ERK), p38, phosphorylated p38 (p-p38), AP-1, MMP-1, NF-κB were obtained from Service Biotechnology Co., Ltd (Wuhan, China). All other reagents used in this study were analytical grade and purchased from Kelong Chemical Reagent Factory (Chengdu, China).

2.2. Sample preparation of PSP-AE

Purple sweet potato was collected from Chongqing, China. The sample was freeze-dried for 24 h and crushed by Chinese herbal medicine crusher (ZS-16, Zhaoshen Electrical Appliance Co., Ltd., China) sieving for a 60 mesh. The powder was stored in the dark and dry place until required.

PSP-AE was extracted according to a previous report (Zhu et al., 2016). The dried purple sweet potato (1.0 g) was blended with 35 mL of 80% ethanol solution (pH = 3) in 100 mL centrifuge tube. PSP-AE was extracted by an ultrasonic processor (KQ3200DE, Kunshan Ultrasonic Instrument Inc., China) at the power of 105 W at 58 °C for 6 min. Thereafter the mixture was centrifuged at 3000 rpm for 5 min and the supernatant was collected. Residue was extracted again under the same conditions. All the supernatants were mixed up, filtered and dried by vacuum evaporation at 45 °C. The total anthocyanin content of PSP-AE was determined by classical pH differential method (Lee, Durst, & Wrolstad, 2005) (may briefly describe the process) and stored at −80 °C until analysis.

2.3. Identification of PSP-AE using UPLC-QTOF-MS

The components of PSP-AE were identified by UPLC-QTOF-MS using a previous method with a slight modification (Li, Zhang, Chen, & Fu, 2017). The analysis was performed on an ACQUITY-UPLC I-Class-G2-XS-QTOF (Waters Co., USA). The ACQUITY UPLC BEH C_{18} column (2.1 × 100 mm i.d, 1.7 μm) was used for separation. The column temperature was 30 °C and the injection volume was 2.0 μL. Mobile phases were acetonitrile (A) and 0.1% formic acid (B), respectively, and the flow rate was 0.25 mL/min. The elution gradients were as follows: 0–1 min, 5% A; 1–6 min, 5–65% A; 6–18 min, 65–100% A; 18–20 min, 100–25% A. The chromatograms of PSP-AE were monitored at 528 nm. The mass spectra were generated in positive-ion mode ranging from *m/z* 100 to 1000. The electrospray ionization (ESI) parameters were as follows: source temperature 120 °C, desolvation temperature 400 °C, capillary voltage 1.5 kV, cone voltage 40 V, cone gas flow 10 L/h, desolvation gas flow 900 L/h. Data were collected and analysis using MassLynx V4.1.

2.4. Animal treatment and UVB irradiation

Thirty-six female BALB/c-nu mice (six weeks old, weight range at 17 ± 1 g) were obtained from the Hunan Slake Jingda Laboratory Animal Co., Ltd (Changsha, China) and randomly divided into six groups. All mice were housed under the standard conditions (25 °C, 55% relative humidity) for a week before the experiment. Mice were subject to one of the following conditions for 8 weeks: Normal control group (oral administration of 0.9% saline, NC); (2) Model control group (UVB irradiation with oral administration of 0.9% saline, MC); (3) Positive control group (UVB irradiation with administration of 50 mg/kg bw V_E, PC); (4) low dose of PSP-AE group (UVB irradiation with administration of 12.5 mg/kg bw PSP-AE, A-L); (5) medium dose of PSP-AE group (UVB irradiation with administration of 25 mg/kg bw PSP-AE, A-M); (6) high dose of PSP-AE group (UVB irradiation with administration of 100 mg/kg bw PSP-AE treatment, A-H). UVB-irradiated was performed 1 h before oral administration using the method reported by Lee et al. (2014). The UVB source was provide by a parallel arrangement of two ultraviolet lamps with 313 nm irradiance peak. Lamps were positioned at a distance of 30 cm above the mice. Mice were daily exposed to different UVB irradiation, and the dosage of irradiation was shown in Table 1.

2.5. The water content determination

The water content of dorsal skin was determined according to a previous report (Ye et al., 2018). The mice were killed by cervical

Table 1
The dosages of irradiation varied during the whole experiment.

No.	Dosage (mJ/cm^2)	Time (min)	Frequency
Week 1	100	10	7
Week 2	200	20	3
Week 3	300	30	3
Week 4–8	400	40	3

vertebra and then the skin tissue was collected. The dorsal skin was dried at 105 °C for 4 h in the oven and then the weight loss was determined. The water content of skin was calculated by the formula as the following: the water content of skin (%) = $(m_1 - m_2)/m_2$. Where $m_1$is the wet weight of skin, and m_2 is the dry weight of skin after 4 h drying.

2.6. Histological examinations

The skin tissue was collected from the mid-dorsal region of the hairless mice and fixed in 4% neutral formaldehyde fixative for over 24 h. The tissue was dehydrated by gradient elution of ethanol, embedded in paraffin, and cut into a thickness of 4 μm. The sections were stained with hematoxylin and eosin (H&E) for assessment of epidermal hyperplasia, and masson's trichrome for evaluation of collagen deposition. Stained sections were observed under the optical microscope (ECLIPSE E100, Nikon Inc., Japan) and quantified by the Image-pro plus 6.0 software.

2.7. Hydroxyproline content estimation

The content of hydroxyproline (Hyp) in skin was measured using the Hyp assay kit according to the manufacturer's instruction.

2.8. SOD, CAT, GSH-Px and MDA determination

The dorsal skin tissues were homogenized with 0.9% physiological saline (1/9, m/v), and then centrifuged at 2500 rpm for 10 min at 4 °C. The supernatants were collected to evaluate the SOD, CAT and GSH-Px activities and MDA levels, which were measured using the correlative test kits according to the manufacturer's instruction.

2.9. Immunohistochemistry analysis

The dorsal skin tissues were fixed in 4% neutral formaldehyde fixative, dehydrated by gradient elution of ethanol, embedded in paraffin, and cut into a thickness of 4 μm. After rehydration and antigen repair, the skin sections were put into 3% hydrogen peroxide to block endogenous peroxidase and incubated with 3% BSA to block non-specific binding site. Thereafter, the sections were incubated with primary antibodies (anti-TNF-α and anti-IL-6) at 4 °C overnight. The secondary antibody was added to the washed tissue sections incubated for 50 min at room temperature. After phosphate buffer saline (PBS) washing, the sections were stained with DAB solution and counter-stained with hematoxylin. Subsequently, the sections were dehydrated, mounted, observed under the optical microscope (ECLIPSE E100, Nikon Inc., Japan) and quantified by the Image-pro plus 6.0 software.

2.10. Immunofluorescence analysis

Quantitative analysis of ROS production was assessed using immunofluorescence experiment. The skin samples were embedded in OCT and sectioned at 8–10 μm. Skin sections were stained with ROS dye solution and incubated for 30 min at 37 °C. Then, sections were washed in PBS solution and stained with DAPI for 10 min. After washing, the sections were mounted, imaged by fluorescence microscope (ECLIPSE C1, Nikon Inc., Japan) and quantified by the Image-pro plus 6.0 software.

2.11. Western blotting

The dorsal skin of mice was homogenized in pre-cold RIPA buffer solution (freshly added protease inhibitor) and centrifuged at 12,000*g* for 10 min at 4 °C. The supernatant collected was total cell lysate. The cytoplasmic and nuclear cytoplasmic proteins were prepared using protein extraction kits according to the manufacturer's instructions. The protein concentration was determined by BCA assay kits. The proteins, applied to 10% SDS-PAGE and separated electrophoretically, were subsequently transferred to a polyvinylidene fluoride (PVDF) membrane (IPVH00010, Millipore Inc., USA). The membranes were blocked in 5% dried skimmed milk for 60 min. Then the membranes were incubated with primary antibodies (anti-JNK, anti-ERK, anti-p38, anti-phosphorylated-JNK, anti-phosphorylated-ERK, anti- phosphorylated-p38, anti-AP-1, anti-MMP-1 or anti-NF-κB) and horseradish peroxidase (HRP)-conjugated secondary antibodies (goat anti-rabbit or goat anti-mouse), respectively. The protein bands were visualized by enhanced chemiluminescence reagent and quantified by AlphaEaseFC software. The GAPDH and Histone H3 were used as internal standards.

2.12. Statistical analysis

All values were repeated at least three times and results were presented as mean ± standard deviations (mean ± SD). The data of statistical analysis were performed by one-way analysis of variance (ANOVA) followed by Duncan's multiple comparison test using SPSS 19.0 statistical analysis software. A p value less than 0.05 was defined as statistically significant.

3. Results

3.1. Determination and identification of PSP-AE

The total anthocyanin content of purple-fleshed sweet potato extracts (PSP-AE) was 134.097 ± 12.484 mg/g. Peak identification and assignment in UPLC fingerprints of PSP-AE were accomplished by comparing with published mass spectral data (He et al., 2016; Lee, Park, Choi, & Jung, 2013). Six anthocyanins of PSP-AE were identified as cyanidin 3-*p*-hydroxybenzoylso-phoroside-5-gluscoside, peonidin 3-*p*- hydroxybenzoylsophoroside-5-gluscoside, cyanidin 3-caffeoylsophoroaide-5-glucoside, cyanidin 3-feruloylsophoroaide-5-glucoside, peonidin 3- caffeoylsophoroaide-5-glucoside and peonidin 3-feruloylsophoroaide-5- glucoside (Supplementary Fig. 1 & Table 2).

Supplementary data associated with this article can be found, in the online version, at https://doi.org/10.1016/j.jff.2019.103640.

3.2. Effect of PSP-AE on macroscopic appearance in mice skin

As shown in Fig. 1A, the macroscopic appearance of skin in NC group was smooth, non-wrinkle, non-invasive, elastic and no relaxation. After eight weeks exposure to UVB irradiation, the skin in MC

Table 2
Retention time (Rt), molecular formulas, molecular mass and fragments of six compounds from PSP-AE.

No.	Rt (min)	Molecular formulas	$[M]^+$ m/z	MS fragment m/z	Compound
1	2.91	$C_{40}H_{45}O_{23}$	893	731,449,287	Cyanidin 3-*p*-hydroxybenzoylsophoroside-5-gluscoside
2	3.09	$C_{41}H_{47}O_{23}$	907	745,463,301	Peonidin 3-*p*-hydroxybenzoylsophoroside-5-gluscoside
3	3.19	$C_{42}H_{47}O_{24}$	935	773,449,287	Cyanidin 3-caffeoylsophoroaide-5-glucoside
4	3.32	$C_{43}H_{49}O_{24}$	949	787,449,287	Cyanidin 3-feruloylsophoroaide-5-glucoside
5	3.52	$C_{43}H_{49}O_{24}$	949	907,463,301	Peonidin 3-caffeoylsophoroaide-5-glucoside
6	3.65	$C_{44}H_{51}O_{24}$	963	463,301	Peonidin 3-feruloylsophoroaide-5-glucoside

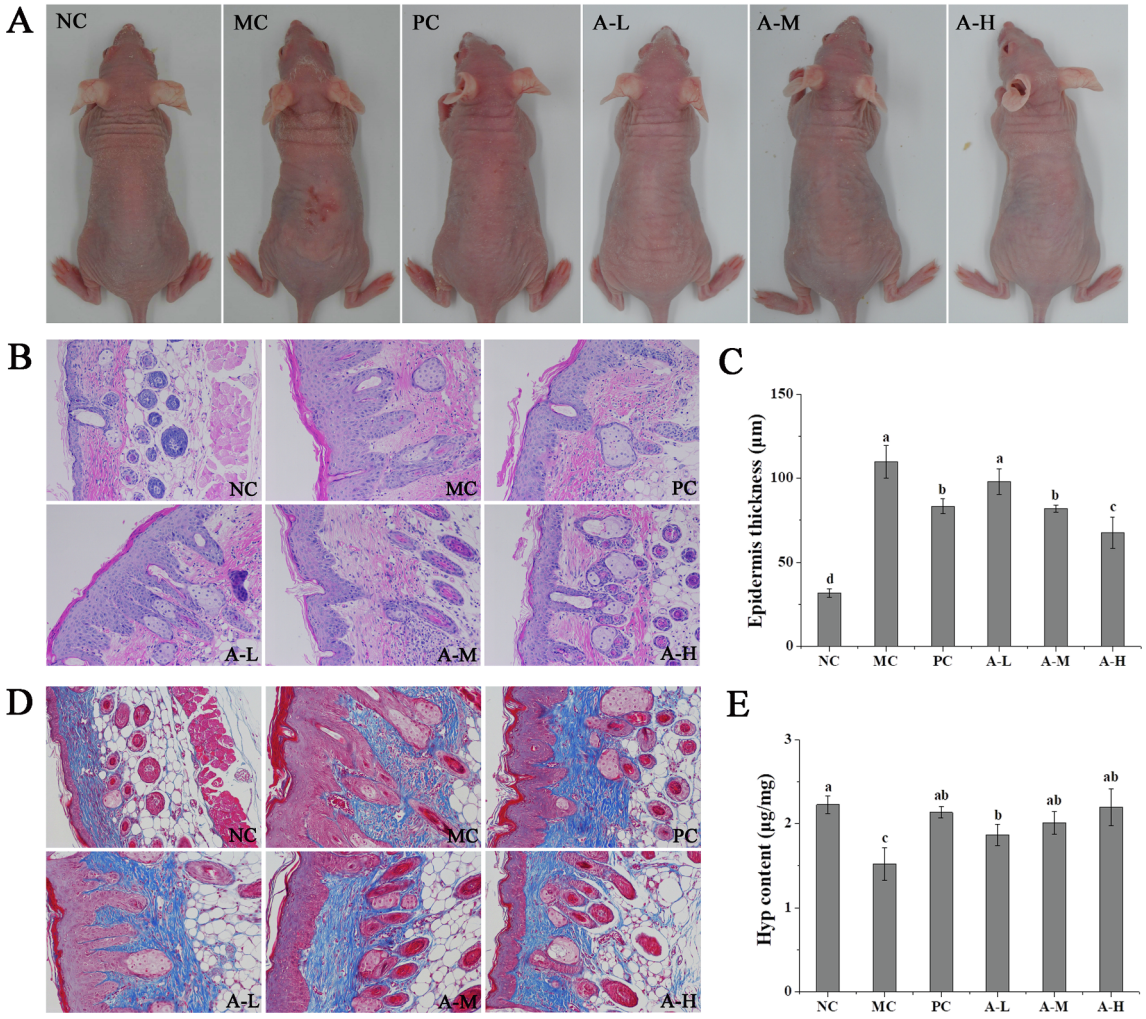

Fig. 1. Effect of PSP-AE on macroscopic and histological changes of BALB/c-nu mice dorsal skin. (A) Skin macroscopic appearances. (B) H&E staining (Magnification, 200×). (C) Epidermal thickness. (D) Masson's trichrome staining (Magnification, 200×). (E) Hyp content. Data were presented as mean ± SD (n = 6). Data with different letters in the same chart implied significant difference ($p < 0.05$).

Table 3
Effect of PSP-AE on the dorsal skin hydration and biochemistry in BALB/c-nu mice.

Group	Dosage (mg/kg)	Hydration (%)	SOD (U/mg prot)	CAT (U/mg prot)	GSH-Px (U/mg prot)	MDA (nmol/mg prot)
NC	–	70.36 ± 4.63^{a}	48.63 ± 3.93^{a}	2.12 ± 0.15^{a}	48.74 ± 3.57^{a}	3.61 ± 0.06^{b}
MC	–	62.93 ± 2.93^{b}	33.53 ± 3.03^{c}	1.05 ± 0.15^{d}	43.13 ± 1.98^{b}	4.73 ± 0.19^{a}
PC	50	72.02 ± 2.96^{a}	44.36 ± 4.13^{ab}	1.59 ± 0.25^{bc}	49.69 ± 1.87^{a}	1.64 ± 0.22^{d}
A-L	12.5	64.20 ± 0.66^{b}	39.15 ± 0.34^{bc}	1.41 ± 0.16^{bd}	42.67 ± 0.53^{b}	2.19 ± 0.25^{c}
A-M	25	67.88 ± 2.47^{ab}	43.87 ± 1.69^{ab}	1.77 ± 0.18^{abc}	50.20 ± 1.68^{a}	1.71 ± 0.04^{d}
A-H	100	70.29 ± 2.08^{a}	48.54 ± 4.07^{a}	1.91 ± 0.16^{ab}	52.30 ± 2.99^{a}	1.50 ± 0.12^{d}

Data were presented as mean ± SD (n = 6). Data with different letters in the same column implied significant difference ($p < 0.05$).

group showed dry, rough, erythema, coarse wrinkle and laxity, and even like leather in appearance and slight damage with surface. Nevertheless, the UVB induced the skin macroscopic changes were ameliorated in PC group and groups treated with PSP-AE. It indicated that PSP-AE administration could reduce the skin wrinkles, recover ruddy gloss appearance, decrease erythema and even alleviate the damage phenomenon. Additionally, the water contents of PC group and A-H group as shown in Table 3 were remarkably increased when compared with that in MC group ($p < 0.05$). Although the A-L and A-M groups showed no significant difference compared with MC group ($p > 0.05$), the water content of skin in these two groups were increased. It indicated that PSP-AE tended to inhibit the UVB-irradiated the macroscopic skin damage and improve the skin hydration degree.

3.3. Effects of PSP-AE on histological changes in mice skin

Continuous UVB irradiation in skin leads to skin inflammation erythema and epidermal thickness (Lee et al., 2014). In order to study the effect of PSP-AE on skin histochemical changes under UVB irradiation, the skin tissue samples were subjected to H&E staining. As exhibited in Fig. 1B, the NC group showed thin epidermis and a wave dermal-epidermal junction. UVB irradiation resulted in epidermis layer

thickening, dermal-epidermal junction damaging and even inflammatory infiltrates occurring, indicating that UVB induced the photoaging in mice skin. By comparison, the pretreatment with PSP-AE ameliorated the damages of skin structure induced by UVB exposure, where A-H group showed the same skin histological changes compared to PC group.

Since the epidermal thickness was used to evaluate the skin photoaging and inflammation as a quantitative parameter (Kim, Song, et al., 2012), we assessed the changes in epidermal thickness of UVB-induced the mice dorsal skin. As exhibited in Fig. 1C, the epidermal thickness in MC group showed significantly increased compared with NC group ($p < 0.05$). The pretreatment with PSP-AE could ameliorate the thickening of epidermal layer, exerting the inhibitory effect on UVB-induced the epidermal hyperplasia.

3.4. Effect of PSP-AE on collagen changes in mice skin

Collagen is a major component of dermal layer in skin, which plays an important role in maintaining the skin structure (Berneburg, Plettenberg, & Krutmann, 2000). In order to visualize the collagen changes in the dermal layer, the skin tissue samples were subjected to masson's trichrome staining. As revealed in Fig. 1D, the skin collagen fibers in MC group showed loose, irregular, and erratically arranged when compared with the closely interweaved and evenly distributed fibers in NC group. However, the morphology of collagen fiber was less damaged in PSP-AE treatment groups than that in MC group.

Hydroxyproline (Hyp), regarded as one of the parameters to evaluate the degree of skin aging, could directly reflect the collagen fibers changes in the dermis (Song, Zhang, Zhang, & Li, 2017). As exhibited in Fig. 1E, the Hyp content in MC group was significantly decreased compared with NC group ($p < 0.05$), while administration of PSP-AE could significantly reverse the reduction of Hyp content triggered by UVB in a dose-dependent manner ($p < 0.05$).

3.5. Effect of PSP-AE on SOD, CAT, GSH-Px and MDA levels in mice skin

Oxidative stress is related with excessive ROS generation and DNA damage. The antioxidant enzymes such as SOD, CAT and GSH-Px can scavenge redundant ROS and restore the body defense (Kim, 2016). Compared with NC group, the SOD, CAT and GSH-Px antioxidant enzymes in MC group were significantly decreased by 31.05%, 50.47% and 11.51%, respectively (Table 3). These three main antioxidant enzymes in A-L group showed no significant difference compared with MC group, while the decreased activities of enzymes induced by UVB were progressively recovered in the A-M and A-H group ($p < 0.05$).

Lipid peroxidation reduced by ROS is regarded as one of the major parameters of oxidative damage, and MDA is the by-product of lipid peroxidation (Kim, 2016). As shown in Table 3, MDA level in MC group was significantly increased by 31.02% compared with NC group. In the three PSP-AE treatment groups, the increased skin MDA levels induced by UVB were significantly suppressed by 53.70%, 63.85% and 68.29%, respectively ($p < 0.05$). Results indicated that PSP-AE effectively reduced the oxidative stress in the skin through improvement of antioxidant enzyme activities and lipid peroxidation.

3.6. Effect of PSP-AE on ROS generation in mice skin

UVB-induced ROS generation plays an important role in the skin photoaging (Bae et al., 2017). The immunofluorescence experiment was used to evaluate the ROS generation and the ROS levels were expressed as average optical. Red[1] represented positive expression and blue represented nucleus in images of skin tissue immunofluorescence study. As illustrated in Fig. 2A and B, the ROS level in MC group was significantly increased more than twice compared with that in NC group. However, the A-M group and A-H group showed significantly inhibitory effect of ROS generation by 21.05% and 35.22% ($p < 0.05$). No statistically significant difference was discovered in PSP-AE-L group. It indicated that PSP-AE could limit the ROS generation to protect the skin against oxidative stress.

3.7. Effect of PSP-AE on TNF-α and IL-6 expressions in mice skin

The effect of PSP-AE on UVB-induced the expression and distribution of pro-inflammatory cytokines in mice skin including TNF-α and IL-6 were investigated. TNF-α and IL-6 positive signals were brown in images of skin tissue immunohistochemistry study. The results revealed that the levels of TNF-α (Fig. 2C and D) and IL-6 (Fig. 2E and F) were significantly enhanced in MC group than those in NC group ($p < 0.05$). However, compared with the MC group, the levels of TNF-α and IL-6 were significantly reduced in PSP-AE treatment in a dose-dependent effect ($p < 0.05$). It indicated that PSP-AE could reduce the inflammatory response to protect the skin against photoaging.

3.8. Effect of PSP-AE on MAPK signaling pathway in mice skin

As showed in Fig. 3A–C, the results indicated that UVB exposure increased the phosphorylation of JNK (p-JNK), ERK (p-ERK) and p38 MAPK (p-p38) proteins compared with NC group. However, compared with MC group, the UVB-induced the expressions of p-JNK, p-ERK and p-p38 proteins were markedly inhibited by the administration of PSP-AE especially in A-H group ($p < 0.05$). Furthermore, the expressions of total proteins of JNK, ERK and p38 MAPK were not changed in each treatment group.

As seen in Fig. 3D, MMP-1 level in MC group increased 3.11-fold higher than that in NC group. However, compared with MC group, the MMP-1 level in A-H group was remarkably decreased by 45.79% ($p < 0.05$). Although the MMP-1 levels in A-L and A-M groups showed no significant difference compared with MC group ($p > 0.05$), they still enable to reduce by 14.21% and 23.11%. Therefore, PSP-AE could suppress the expression of MMP-1 and sustain the stability of collagen structure to protect the skin from UVB-induced the photoaging.

3.9. Effect of PSP-AE on NF-κB expression in mice skin

NF-κB is a downstream target of the MAPK signal pathway (Divya et al., 2015). As illustrated in Fig. 3F, the nuclear level of NF-κB in MC group was significantly enhanced compared with that in NC group. While all the PSP-AE treatment groups significantly inhibited the nuclear translocation of NF-κB expression by 26.28%, 34.06% and 60.28%, respectively. The inhibitory effect of PSP-AE on UVB-induced the translocation of NF-κB from cytoplasm to nucleus could prevent skin from inflammation invade.

4. Discussion

This study was designed to investigate the chemopreventive effect of PSP-AE against UVB-induced photoaging and explore the underlying mechanisms using the BALB/c-nu mouse skin model. It is well known that prolonged exposure to UVB irradiation lead to skin photoaging accompanied by the formation of skin dryness, roughness, wrinkles and laxity (Lee et al., 2018). The major cause of skin photodamage is the degradation and destruction of the collagen, which is the main structural component of extracellular matrix (ECM) in skin dermis (Kong et al., 2018). Hydroxyproline (Hyp), a specific amino acid of skin collagen, possesses to promote the regeneration of collagen and repair the metabolic damage of skin, which is regarded as a quantitative index to evaluate the level of collagen (Kong et al., 2018). The overexpression of matrix metalloproteinases (MMPs) can degrade ECM including collagen

[1] For interpretation of color in Fig. 2, the reader is referred to the web version of this article.

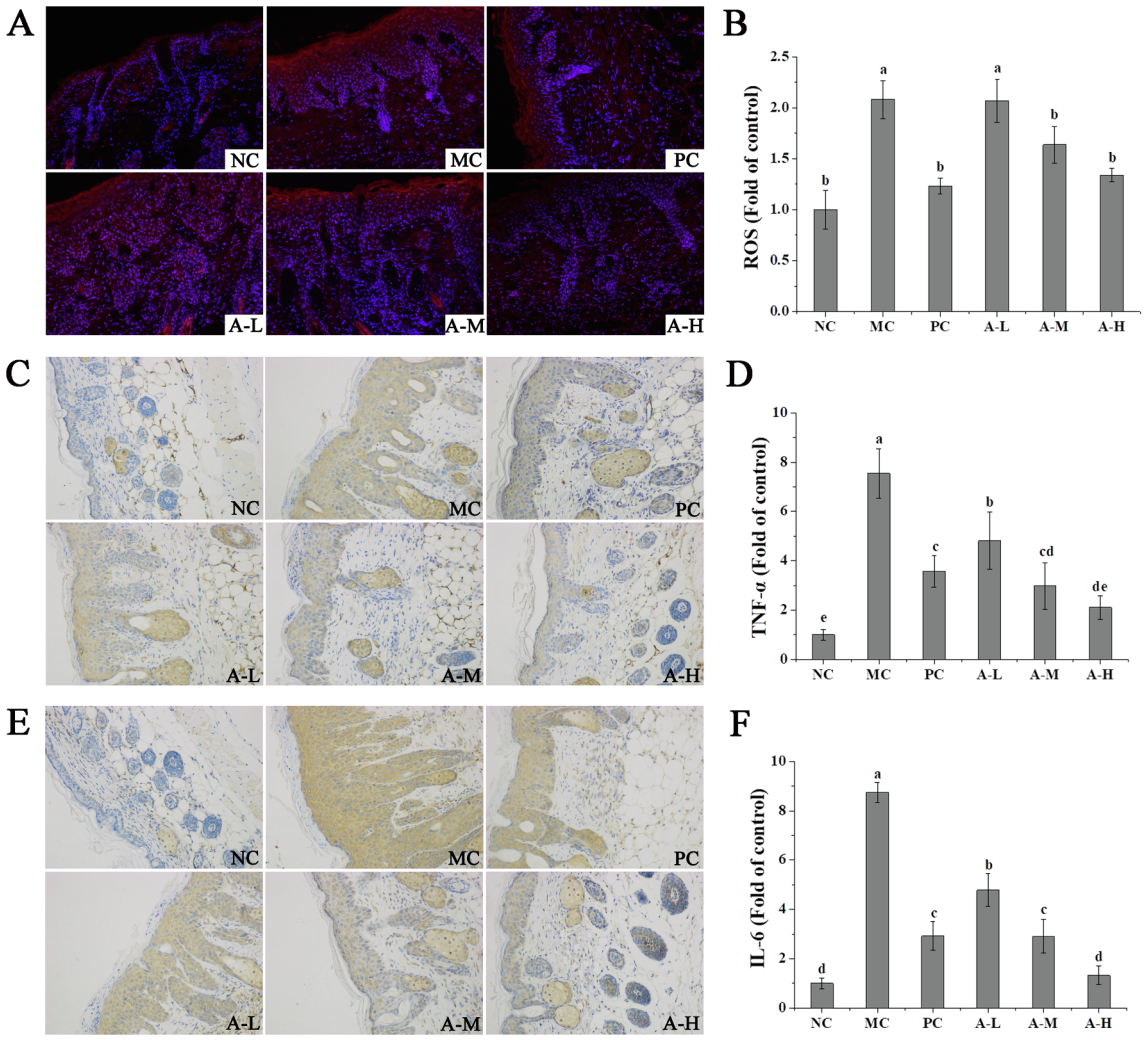

Fig. 2. Effect of PSP-AE on the immunofluorescence and immunohistochemistry analysis in BALB/c-nu mice dorsal skin. (A) The immunofluorescence sections of ROS. (B) The quantitative analysis of ROS level. (C) The immunohistochemistry sections of TNF-α. (D) The quantitative analysis of TNF-α expression. (E) The immunohistochemistry analysis of IL-6. (F) The quantitative analysis of IL-6 expression. Quantitative analysis of expression intensity was performed by Image-pro plus 6.0 software. Data were presented as mean ± SD (n = 6). Data with different letters in the same chart implied significant difference ($p < 0.05$).

fibers, which are responsible for the formation of skin wrinkle and laxity (Shah & Rawal Mahajan, 2013). In addition, inhibition of skin hydration caused by UVB irradiation can make skin dull and coarse in appearance, and irregular thickening of skin epidermis called epidermal hyperplasia can cause skin wrinkle and roughness. In this study, typical photoaging characteristics were observed after UVB irradiation for eight weeks, such as dryness, rough, erythema, coarse wrinkle and laxity in macroscopic appearance. Histological analysis revealed that the epidermal thickness of the mice dorsal skin was remarkably increased and the collagen fibers showed sparseness and disorder. Additionally, UVB induced skin hydration and Hyp content were significantly decreased compared with control group. However, PSP-AE treatment especially at dose of 100 mg/kg bw effectively reduced the UVB-induced skin adverse changes such as inhibition of epidermal hyperplasia, improvement of skin hydration, recovery of collagen fibers and evaluation of Hyp content. Moreover, PSP-AE significantly inhibited the protein expression of MMP-1. It indicated that PSP-AE could display the protective effect against UVB-induced photoaging.

Generally, the human body possesses three antioxidant enzymes including SOD, GSH-Px and CAT, which act as the first antioxidant defense system to scavenge excessive free radicals and repair oxidative damage (Popovic et al., 2017). Accumulated evidences have demonstrated the pathogenesis of UVB-induced photodamage is related to oxidative stress accompanied by excessive generation of ROS (Bosch et al., 2015; Jensen, Wing, & Dellavalle, 2010), which seriously destroyed the skin antioxidant defense system. Lipid peroxidation is an important source of oxidative stress and significantly increased in UVB-irradiated the mice skin (Divya et al., 2015). MDA, the degradation product of lipid peroxidation triggered by UVB, is widely regarded as one of important biological markers of oxidative stress (Del Rio, Stewart, & Pellegrini, 2005). In the present study, we observed that PSP-AE could significantly ameliorate UVB-induced decreasing in SOD, CAT, GSH-Px antioxidant enzymes activities and increasing in the level of MDA. The beneficial effect of PSP-AE might involve the inhibition of UVB irradiated ROS overproduction.

Mitogen-activated protein kinases (MAPKs), acting as important regulators of extracellular signals from cell surface to nucleus including JNK, ERK and p38, play a major role in cellular differentiation, proliferation and apoptosis (Sharma, Meeran, & Katiyar, 2007). Previous studies have confirmed that UVB-induced oxidative stress plays an important role in activating the MAPK pathway (Chiang, Chan, Chu, & Wen, 2015; Lu, Hou, Fan, Yang, & Li, 2017). ERK is primarily activated by growth factor receptors, while JNK and p38 are activated by cytokine receptors and various environmental stimuli such as UV irradiation (Fisher et al., 1998). The transcription factor of activator protein-1 (AP-1), an important downstream regulator of JNK and p38 MAPK, is

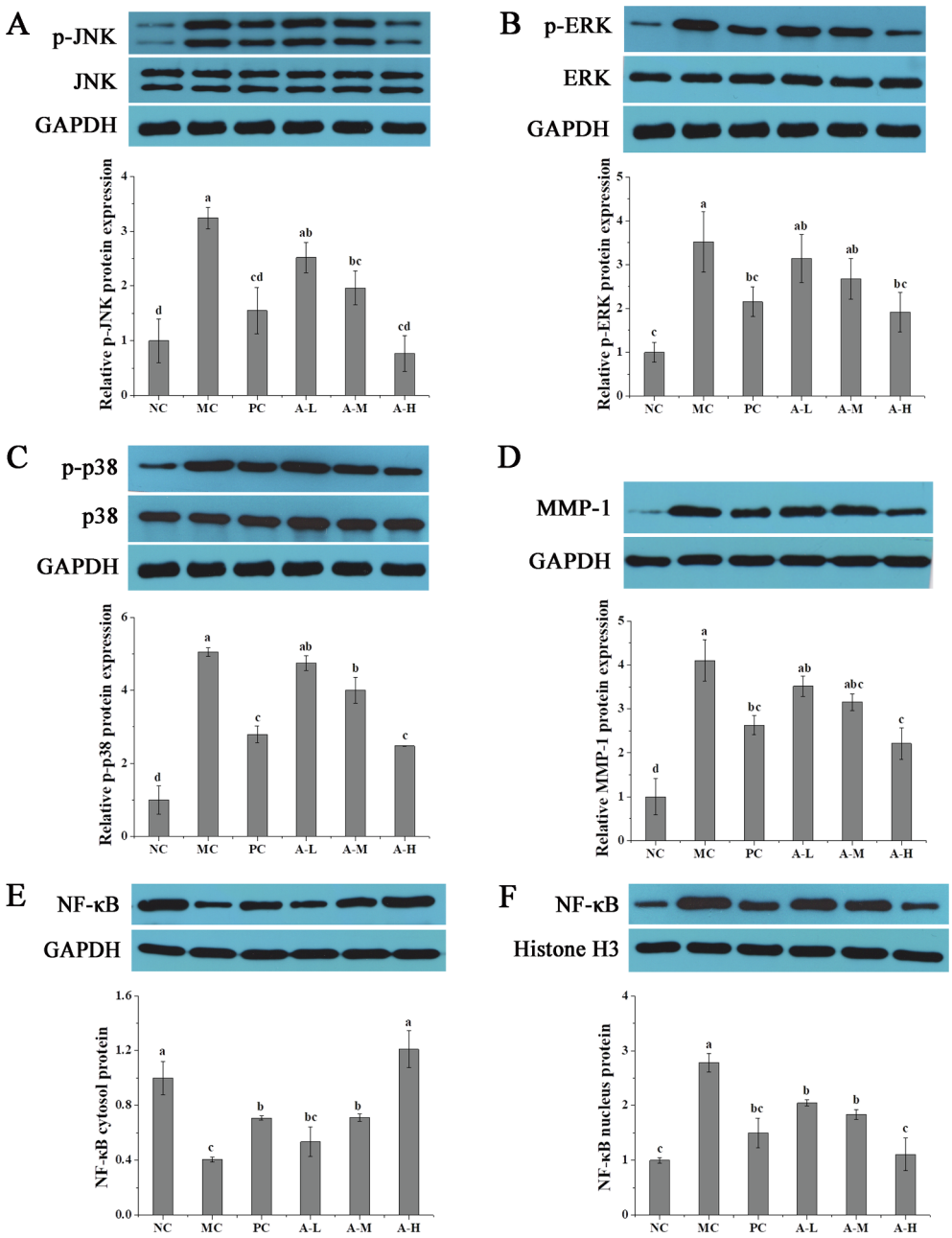

Fig. 3. Effect of PSP-AE on the protein expressions in BALB/c-nu mice dorsal skin. (A) Phosphorylation expression of JNK protein. (B) Phosphorylation expression of ERK protein. (C) Phosphorylation expression of p-p38 protein. (D) The expression of MMP-1 protein. (E) The expression of NF-κB cytosol protein. (F) The expression of NF-κB nucleus protein. The relative density of each band was performed as a fold- change compared with normal control group. Data were presented as mean ± SD (n = 6). Data with different letters in the same chart implied significant difference ($p < 0.05$).

regulated by MAPKs proteins and involved in various biological process including UVB-induced skin inflammation (Yoon et al., 2011). Previous studies have reported that UVB-induced the oxidative stress mediates the levels of phosphorylation of MAPKs including JNK, ERK and p38, which are responsible for photoaging (Choi, Kundu, Chun, Na, & Surh, 2014; Sun et al., 2016). However, no studies have yet confirmed that anthocyanins could exert anti-photoaging effects *via* inhibiting MAPK signaling pathway. In this study, we found that PSP-AE could significantly suppress the UVB-induced the phosphorylation of MAPKs proteins, such as JNK, ERK and p38 in mice skin. Therefore, the study suggested that PSP-AE might inhibit UVB induced the activation of MAPK signaling pathway by suppressing UVB-induced oxidative stress, which is an important target for prevention and treatment of photoaging.

It has been reported that phosphorylation of MAPK proteins can mediate the downstream events, such as AP-1 and NF-κB (Sun et al., 2016). ERK and p38 MAPK proteins have been shown to regulate the activation of NF-κB (Sharma & Katiyar, 2010). NF-κB, a transcription factor, plays a vital role in various stages of tumors and carcinogenesis, which can be activated by agents including UVB irradiated the generation of ROS (Khan, Syed, Pal, Mukhtar, & Afaq, 2012). Previous studies have demonstrated that skin inflammation induced by prolonged UVB-irradiation was related to the development of skin photoaging (Han et al., 2018; Li, Lin, Lu, Zhou, & Luo, 2016). Activation of NF-κB can up-regulate the pro-inflammatory cytokines expressions, including TNF-α and IL-6. TNF-α and IL-6 are regarded as important regulators of inflammation intensity (Wagener, Carels, & Lundvig, 2013). Accumulated reports have shown that inhibiting the activation

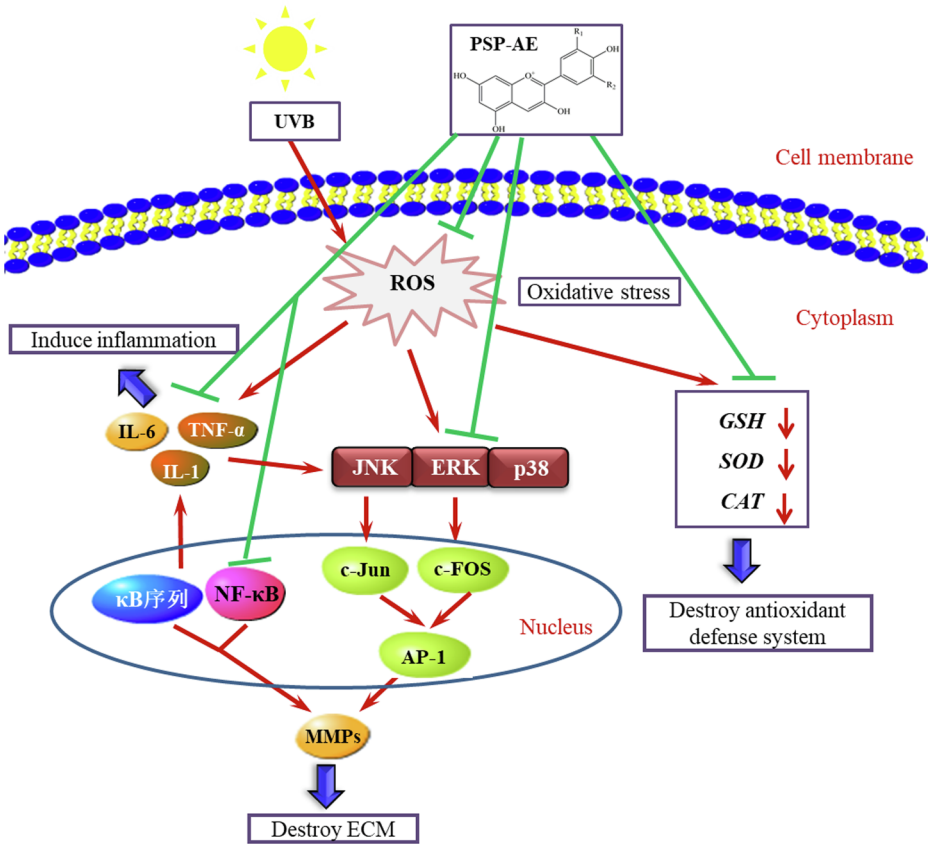

Fig. 4. The possible mechanisms of the mice skin anti-photoaging effect of PSP-AE. ROS: reactive oxygen species; TNF-α: tumor necrosis factor-α; IL-6: interleukin-6; JNK: c-Jun N-terminal kinase; ERK: extracellular regulated protein kinases; GSH-Px: glutathione peroxidase; SOD: superoxide dismutase; CAT: catalase; AP-1: activator protein 1; MMPs: matrix metalloproteinase; ECM: extracellular matrix.

of NF-κB is one of important mechanisms of plant phenolics against photoaging, such as proanthocyanidins, astragaloside and caffeic acid (Kim et al., 2013; Sharma et al., 2007; Yang et al., 2011). In this study, PSP-AE treatment effectively inhibited the over-expression of TNF-α and IL-6, and suppressed the activation and translocation of NF-κB to the nucleus in the UVB irradiated mice skin. Therefore, our results suggested that PSP-AE could prevent skin from UVB-induced inflammatory response by inhibiting the expression of pro-inflammatory cytokines and interrupting the nuclear translocation of NF-κB.

MMP-1 plays an important role in degrading extracellular matrix and destroying the collagen structure (Chiang et al., 2015; Lu et al., 2017). MAPK and NF-κB signaling pathways can regulate the MMPs expression (Kim, Kim, Yun, & Hwang, 2017). Previous studies reported that the activation of MAPK and NF-κB are responsible for stimulating and accelerating the expression of MMP-1 (Kim et al., 2013; Sun et al., 2016). In the present study, UVB-induced MMP-1 expression was attenuated by PSP-AE treatment, which was mediated by inhibiting the phosphorylation of MAPK proteins and translocation of NF-κB to the nucleus (Fig. 4). Collectively, the MAPK and NF-κB signaling pathways might be the potential targets for mediating the expression of MMPs in BALB/c-nu mouse model, which plays an important role in the protective effect of PSP-AE against the photodamage.

5. Conclusion

Our study demonstrated that the anthocyanin extracts from purple-fleshed sweet potato could ameliorate the UVB-induced water loss, collagen degradation, epidermal hyperplasia and wrinkle formation. It was probably mediated by inhibiting the UVB-induced oxidative stress and inflammatory response as well as MMP-1 expression *via* modulating MAPK and NF-κB signaling pathways. Therefore, the purple-fleshed sweet potato anthocyanin extracts might be a potential skin anti-photoaging agent for skin health.

Conflict of interest

On behalf of all the authors, the corresponding author states that there is no conflict of interest.

Acknowledgement

This research project was financially supported by National Natural Science Foundation of China (31771970), Fundamental Research Funds for the Central Universities of China (XDJK2018B030), and Chongqing Science and Technology Foundation (cstc2015shms-ztzx80006).

References

Bae, J., Han, M., Shin, H. S., Kim, M., Shin, C., Lee, D. H., & Chung, J. H. (2017). *Perilla frutescens* leaves extract ameliorates ultraviolet radiation-induced extracellular matrix damage in human dermal fibroblasts and hairless mice skin. *Journal of Ethnopharmacology, 195*, 334–342.

Berneburg, M., Plettenberg, H., & Krutmann, J. (2000). Photoaging of human skin. *Photodermatology Photoimmunology & Photomedicine, 16*, 239–244.

Bosch, R., Philips, N., Suarez-Perez, J. A., Juarranz, A., Devmurari, A., Chalensouk-Khaosaat, J., & Gonzalez, S. (2015). Mechanisms of photoaging and cutaneous photocarcinogenesis, and photoprotective strategies with phytochemicals. *Antioxidants, 4*, 248–268.

Chiang, H., Chan, S., Chu, Y., & Wen, K. (2015). Fisetin ameliorated photodamage by suppressing the mitogen-activated protein kinase/matrix metalloproteinase pathway and nuclear factor-kappa B pathways. *Journal of Agricultural and Food Chemistry, 63*, 4551–4560.

Cho, S., Lowe, L., Hamilton, T. A., Fisher, G. J., Voorhees, J. J., & Kang, S. (2005). Long-term treatment of photoaged human skin with topical retinoic acid improves epidermal cell atypia and thickens the collagen band in papillary dermis. *Journal of the American Academy of Dermatology, 53*, 769–774.

Choi, K., Kundu, J. K., Chun, K., Na, H., & Surh, Y. (2014). Rutin inhibits UVB radiation-induced expression of COX-2 and iNOS in hairless mouse skin: p38 MAP kinase and JNK as potential targets. *Archives of Biochemistry and Biophysics, 559*, 38–45.

Del Rio, D., Stewart, A. J., & Pellegrini, N. (2005). A review of recent studies on malondialdehyde as toxic molecule and biological marker of oxidative stress. *Nutrition Metabolism and Cardiovascular Diseases, 15*, 316–328.

Divya, S. P., Wang, X., Pratheeshkumar, P., Son, Y., Roy, R. V., Kim, D., ... Zhang, Z.

(2015). Blackberry extract inhibits UVB-induced oxidative damage and inflammation through MAP kinases and NF-kappa B signaling pathways in SKH-1 mice skin. *Toxicology and Applied Pharmacology, 284*, 92–99.
Fisher, G. J., Talwar, H. S., Lin, J. Y., Lin, P. P., McPhillips, F., Wang, Z. Q., ... Voorhees, J. J. (1998). Retinoic acid inhibits induction of c-Jun protein by ultraviolet radiation that occurs subsequent to activation of mitogen-activated protein kinase pathways in human skin *in vivo*. *Journal of Clinical Investigation, 101*, 1432–1440.
Han, M., Bae, J., Ban, J., Shin, H. S., Lee, D. H., & Chung, J. H. (2018). Black rice (*Oryza sativa* L.) extract modulates ultraviolet-induced expression of matrix metalloproteinases and procollagen in a skin cell model. *International Journal of Molecular Medicine, 41*, 3073–3080.
Han, S., Kang, S. M., Oh, J., Lee, D. H., & Chung, J. H. (2018). Src kinase mediates UV-induced TRPV1 trafficking into cell membrane in HaCaT keratinocytes. *Photodermatology Photoimmunology & Photomedicine, 34*, 214–216.
He, W., Zeng, M., Chen, J., Jiao, Y., Niu, F., Tao, G., ... He, Z. (2016). Identification and quantitation of anthocyanins in purple-fleshed sweet potatoes cultivated in China by UPLC-PDA and UPLC-QTOF-MS/MS. *Journal of Agricultural and Food Chemistry, 64*, 171–177.
Jensen, J. D., Wing, G. J., & Dellavalle, R. P. (2010). Nutrition and melanoma prevention. *Clinics in Dermatology, 28*, 644–649.
Khan, N., Syed, D. N., Pal, H. C., Mukhtar, H., & Afaq, F. (2012). Pomegranate fruit extract inhibits UVB-induced inflammation and proliferation by modulating NF-kappa B and MAPK signaling pathways in mouse skin. *Photochemistry and Photobiology, 88*, 1126–1134.
Khoo, H. E., Azlan, A., Tang, S. T., & Lim, S. M. (2017). Anthocyanidins and anthocyanins: Colored pigments as food, pharmaceutical ingredients, and the potential health benefits. *Food & Nutrition Research, 61*, 1–21.
Kim, D., Shin, G., Kim, J., Kim, Y., Lee, J., Lee, J. S., ... Lee, O. (2016). Antioxidant and anti-ageing activities of citrus-based juice mixture. *Food Chemistry, 194*, 920–927.
Kim, H. K. (2016). Garlic supplementation ameliorates UV-induced photoaging in hairless mice by regulating antioxidative activity and MMPs expression. *Molecules, 21*, 70.
Kim, H. W., Kim, J. B., Cho, S. M., Chung, M. N., Lee, Y. M., Chu, S. M., ... Lee, D. J. (2012). Anthocyanin changes in the Korean purple-fleshed sweet potato, *Shinzami*, as affected by steaming and baking. *Food Chemistry, 130*, 966–972.
Kim, H., Song, J. H., Youn, U. J., Hyun, J. W., Jeong, W. S., Lee, M. Y., ... Chae, S. (2012). Inhibition of UVB-induced wrinkle formation and MMP-9 expression by mangiferin isolated from *Anemarrhena asphodeloides*. *European Journal of Pharmacology, 689*, 38–44.
Kim, J., Kim, M., Yun, J. G., & Hwang, J. (2017). Protective effects of standardized *Siegesbeckia glabrescens* extract and its active compound kirenol against UVB-induced photoaging through inhibition of MAPK/NF-kappa B pathways. *Journal of Microbiology and Biotechnology, 27*, 242–250.
Kim, S. R., Jung, Y. R., An, H. J., Kim, D. H., Jang, E. J., Choi, Y. J., ... Chung, H. Y. (2013). Anti-wrinkle and anti-inflammatory effects of active garlic components and the inhibition of MMPs *via* NF-κB signaling. *PloS One, 8*, e73877.
Kong, S., Li, D., Luo, H., Li, W., Huang, Y., Li, J., ... Li, S. (2018). Anti-photoaging effects of chitosan oligosaccharide in ultraviolet-irradiated hairless mouse skin. *Experimental Gerontology, 103*, 27–34.
Kwak, C. S., Yang, J., Shin, C., & Chung, J. H. (2018). Topical or oral treatment of peach flower extract attenuates UV-induced epidermal thickening, matrix metalloproteinase-13 expression and pro-inflammatory cytokine production in hairless mice skin. *Nutrition Research and Practice, 12*, 29–40.
Kwon, J. Y., Lee, K. W., Kim, J., Jung, S. K., Kang, N. J., Hwang, M. K., ... Lee, H. J. (2009). Delphinidin suppresses ultraviolet B-induced cyclooxygenases-2 expression through inhibition of MAPKK4 and PI-3 kinase. *Carcinogenesis, 30*, 1932–1940.
Lee, H. J., Im, A., Kim, S., Kang, H., Lee, J. D., & Chae, S. (2018). The flavonoid hesperidin exerts anti-photoaging effect by downregulating matrix metalloproteinase (MMP)-9 expression *via* mitogen activated protein kinase (MAPK)-dependent signaling pathways. *Bmc Complementary and Alternative Medicine, 18*, 1–9.
Lee, J., Durst, R. W., & Wrolstad, R. E. (2005). Determination of total monomeric anthocyanin pigment content of fruit juices, beverages, natural colorants, and wines by the pH differential method: Collaborative study. *Journal of Aoac International, 88*, 1269–1278.
Lee, M. J., Park, J. S., Choi, D. S., & Jung, M. Y. (2013). Characterization and quantitation of anthocyanins in purple-fleshed sweet potatoes cultivated in Korea by HPLC-DAD and HPLC-ESI-QTOF-MS/MS. *Journal of Agricultural and Food Chemistry, 61*, 3148–3158.
Lee, T. H., Do, M. H., Oh, Y. L., Cho, D. W., Kim, S. H., & Kim, S. Y. (2014). Dietary fermented soybean suppresses UVB-induced skin inflammation in hairless mice *via* regulation of the MAPK signaling pathway. *Journal of Agricultural and Food Chemistry, 62*, 8962–8972.
Li, F., Zhang, B., Chen, G., & Fu, X. (2017). The novel contributors of anti-diabetic potential in mulberry polyphenols revealed by UHPLC-HR-ESI-TOF-MS/MS. *Food Research International, 100*, 873–884.
Li, M., Lin, X., Lu, J., Zhou, B., & Luo, D. (2016). Hesperidin ameliorates UV radiation-induced skin damage by abrogation of oxidative stress and inflammatory in HaCaT cells. *Journal of Photochemistry and Photobiology B-Biology, 165*, 240–245.
Lu, J., Hou, H., Fan, Y., Yang, T., & Li, B. (2017). Identification of MMP-1 inhibitory peptides from cod skin gelatin hydrolysates and the inhibition mechanism by MAPK signaling pathway. *Journal of Functional Foods, 33*, 251–260.
Masaki, H. (2010). Role of antioxidants in the skin: Anti-aging effects. *Journal of Dermatological Science, 58*, 85–90.
Poon, F., Kang, S., & Chien, A. L. (2015). Mechanisms and treatments of photoaging. *Photodermatology Photoimmunology & Photomedicine, 31*, 65–74.
Popovic, N., Pajovic, B. S., Stojiljkovic, V., Todorovic, A., Pejic, S., Pavlovic, I., & Gavrilovic, L. (2017). Increased activity of hippocampal antioxidant enzymes as an important adaptive phenomenon of the antioxidant defense system in chronically stressed rats. *Acta Veterinaria-Beograd, 67*, 540–550.
Pratheeshkumar, P., Son, Y., Wang, X., Divya, S. P., Joseph, B., Hitron, J. A., ... Shi, X. L. (2014). Cyanidin-3-glucoside inhibits UVB-induced oxidative damage and inflammation by regulating MAP kinase and NF-kappa B signaling pathways in SKH-1 hairless mice skin. *Toxicology and Applied Pharmacology, 280*, 127–137.
Rabe, J. H., Mamelak, A. J., McElgunn, P. J. S., Morison, W. L., & Sauder, D. N. (2006). Photoaging: Mechanisms and repair. *Journal of the American Academy of Dermatology, 55*, 1–19.
Ren, X., Shi, Y., Zhao, D., Xu, M., Li, X., Dang, Y., & Ye, X. (2016). Naringin protects ultraviolet B-induced skin damage by regulating p38 MAPK signal pathway. *Journal of Dermatological Science, 82*, 106–114.
Shah, H., & Rawal Mahajan, S. (2013). Photoaging: New insights into its stimulators, complications, biochemical changes and therapeutic interventions. *Biomedicine & Aging Pathology, 3*, 161–169.
Sharma, S. D., & Katiyar, S. K. (2010). Dietary grape seed proanthocyanidins inhibit UVB-induced cyclooxygenase-2 expression and other inflammatory mediators in UVB-exposed skin and skin tumors of SKH-1 hairless mice. *Pharmaceutical Research, 27*, 1092–1102.
Sharma, S. D., Meeran, S. M., & Katiyar, S. K. (2007). Dietary grape seed proanthocyanidins inhibit UVB-induced oxidative stress and activation of mitogen-activated protein kinases and nuclear factor-kappa B signaling *in vivo* SKH-1 hairless mice. *Molecular Cancer Therapeutics, 6*, 995–1005.
Song, H., Zhang, S., Zhang, L., & Li, B. (2017). Effect of orally administered collagen peptides from bovine bone on skin aging in chronologically aged mice. *Nutrients, 9*, 1209.
Sun, Z., Park, S. Y., Hwang, E., Park, B., Seo, S. A., Cho, J., ... Yi, T. (2016). Dietary *Foeniculum vulgare Mill* extract attenuated UVB irradiation- induced skin photoaging by activating of Nrf2 and inhibiting MAPK pathways. *Phytomedicine, 23*, 1273–1284.
Svobodova, A., Psotova, J., & Walterova, D. (2003). Natural phenolics in the prevention of UV-induced skin damage: A review. *Biomedical Papers (Olomouc), 147*, 137–145.
Uliasz, A., & Spencer, J. M. (2004). Chemoprevention of skin cancer and photoaging. *Clinics in Dermatology, 22*, 178–182.
Wagener, F. A. D. T., Carels, C. E., & Lundvig, D. M. S. (2013). Targeting the redox balance in inflammatory skin conditions. *International Journal of Molecular Sciences, 14*, 9126–9167.
Yang, B., Ji, C., Chen, X., Cui, L., Bi, Z., Wan, Y., & Xu, J. (2011). Protective effect of astragaloside IV against matrix metalloproteinase-1 expression in ultraviolet- irradiated human dermal fibroblasts. *Archives of Pharmacal Research, 34*, 1553–1560.
Ye, Y., Ji, D., You, L., Zhou, L., Zhao, Z., & Brennan, C. (2018). Structural properties and protective effect of *Sargassum fusiforme* polysaccharides against ultraviolet B radiation in hairless Kun Ming mice. *Journal of Functional Foods, 43*, 8–16.
Ye, Y., Sun-Waterhouse, D., You, L., & Abbasi, A. M. (2017). Harnessing food-based bioactive compounds to reduce the effects of ultraviolet radiation: A review exploring the link between food and human health. *International Journal of Food Science and Technology, 52*, 595–607.
Yoon, J. H., Lim, T., Lee, K. M., Jeon, A. J., Kim, S. Y., & Lee, K. W. (2011). Tangeretin reduces ultraviolet B (UVB)-induced cyclooxygenase-2 expression in mouse epidermal cells by blocking mitogen-activated protein kinase (MAPK) activation and reactive oxygen species (ROS) generation. *Journal of Agricultural and Food Chemistry, 59*, 222–228.
Zhu, Z., Guan, Q., Guo, Y., He, J., Liu, G., Li, S., ... Jaffrin, M. Y. (2016). Green ultrasound-assisted extraction of anthocyanin and phenolic compounds from purple sweet potato using response surface methodology. *International Agrophysics, 30*, 113–122.